Acta Phys. Hung. A 19/1 (2004) 000–000

HEAVY ION PHYSICS

1219-7580/04/ $ 20.00

Recent Results from Phobos

Edmundo García[6,a] for the Phobos Collaboration:
B.B.Back[1], M.D.Baker[2], M.Ballintijn[4], D.S.Barton[2], R.R.Betts[6], A.A.Bickley[7], R.Bindel[7], W.Busza[4], A.Carroll[2], Z.Chai[2], M.P.Decowski[4], E.García[6], T.Gburek[3], N.George[2], K.Gulbrandsen[4], C.Halliwell[6], J.Hamblen[8], M.Hauer[2], C.Henderson[4], D.J.Hofman[6], R.S.Hollis[6], R.Hołyński[3], B.Holzman[2], A.Iordanova[6], E.Johnson[8], J.L.Kane[4], N.Khan[8], P.Kulinich[4], C.M.Kuo[5], W.T.Lin[5], S.Manly[8], A.C.Mignerey[7], R.Nouicer[2,6], A.Olszewski[3], R.Pak[2], C.Reed[4], C.Roland[4], G.Roland[4], J.Sagerer[6], H.Seals[2], I.Sedykh[2], C.E.Smith[6], M.A.Stankiewicz[2], P.Steinberg[2], G.S.F.Stephans[4], A.Sukhanov[2], M.B.Tonjes[7], A.Trzupek[3], C.Vale[4], G.J.van Nieuwenhuizen[4], S.S.Vaurynovich[4], R.Verdier[4], G.I.Veres[4], E.Wenger[4], F.L.H.Wolfs[8], B.Wosiek[3], K.Woźniak[3], B.Wysłouch[4]

[1] Argonne National Laboratory, Argonne, IL 60439-4843, USA
[2] Brookhaven National Laboratory, Upton, NY 11973-5000, USA
[3] Institute of Nuclear Physics PAN, Kraków, Poland
[4] Massachusetts Institute of Technology, Cambridge, MA 02139-4307, USA
[5] National Central University, Chung-Li, Taiwan
[6] University of Illinois at Chicago, Chicago, IL 60607-7059, USA
[7] University of Maryland, College Park, MD 20742, USA
[8] University of Rochester, Rochester, NY 14627, USA

Received 1 November 2005

Abstract. The PHOBOS detector is one of four heavy ion experiments at the Relativistic Heavy Ion Collider at Brookhaven National Laboratory. In this paper we will review some of the results of PHOBOS from the data collected in p+p, d+Au and Au+Au collisions at nucleon-nucleon center-of-mass energies up to 200 GeV: Evidence is found of the formation of a very high energy density and highly interactive system, which can not be described in terms of hadrons, and has a relatively low baryon density. There is evidence that the system formed is thermalized to a certain degree. Scaling with the number of participants and extended longitudinal scaling behavior are also observed in distributions of produced charged particles.

Keywords: Heavy ions, RHIC, PHOBOS
PACS: 25.75.-q.25.75.Dw,25.75.Gz

1. Introduction

The bulk of the hadronic matter is made of quarks and gluons (partons), bound into neutrons and protons. The fundamental interactions between partons are well understood at large momentum transfer by the theory of Quantum Chromodynamics (QCD). However, due to the non-commutative nature of the theory, strongly interacting matter is only partially understood in terms of QCD. Thus the only knowledge we can access on the properties of strongly-interacting matter comes from experimental data.

Lattice gauge calculations suggest that at low baryon densities there is a phase transition in a strongly interactive matter below and above a critical temperature $T_c \sim 170$ MeV, corresponding to an energy density $\epsilon \sim 1$ GeV/fm^3 [1]. The closest approach to the creation of matter under these conditions may be achieved in collisions of large nuclei, as studied at the Relativistic Heavy Ion Collider (RHIC). Data from these experiments are being studied to get a better understanding of the physics of heavy-ion collisions and in particular to search for the evidence of a phase transition in strongly-interacting matter. This paper summarizes some of the results obtained by the PHOBOS collaboration.

The PHOBOS apparatus is composed of three major subsystems: a charged particle multiplicity detector covering almost the entire solid angle, a two arm magnetic spectrometer with particle identification capability, and a suite of detectors used for triggering and centrality determination. A full description of the PHOBOS detector and its properties can be found in Ref. [2]. Also, a description of some of the techniques used for the PHOBOS event selection (triggering) and event characterization (vertex position and centrality of the collision) can be found in Ref. [3].

2. The formation of a very high energy density state at RHIC

Figure 1 is the evolution of the midrapidity charged particle density $dN_{ch}/d\eta\rfloor_{|\eta|\leq 1}$, per participating nucleon pair, $N_{part}/2$, as a function of $\sqrt{s_{_{NN}}}$ [4]. The data are consistent with a logarithmic extrapolation from lower energies as shown by the solid line drawn in the plot. The mid rapidity particle density at $\sqrt{s_{_{NN}}}$= 200 GeV is almost a factor of two higher than the value observed at the maximum SPS energy.

An approximation of the total energy density in the system created at midrapidity in Au+Au collisions at $\sqrt{s_{_{NN}}}$=200 GeV can be calculated from the charged particle pseudorapidity density, the average energy per particle and the volume from where the system was originated. Fits to the yield of transverse momentum distributions of identified particles emitted at mid rapidity in central Au+Au collisions at $\sqrt{s_{_{NN}}}$=200 GeV measured by PHOBOS [6] make it possible to estimate the average transverse mass for all charged particles, $\langle m_T \rangle \simeq 600$ MeV/c, which is equal to the transverse energy at midrapidity.

As for the volume where the system originated, elliptic flow results discussed in

Sec. 4 suggest that an upper limit of the time for the system to reach approximate equilibrium is of the order of 1–2 fm/c. Using the upper range of this estimate and assuming that the system expands during this time in both longitudinal and transverse directions one obtains a conservative estimate for the energy density produced at RHIC when the system reaches approximate equilibrium of $\epsilon \geq 3$ GeV/fm^3. This estimate is about 6 times the energy density inside the nucleons. Thus, a very high energy system is created whose description in terms of hadronic degrees of freedom should be inappropriate.

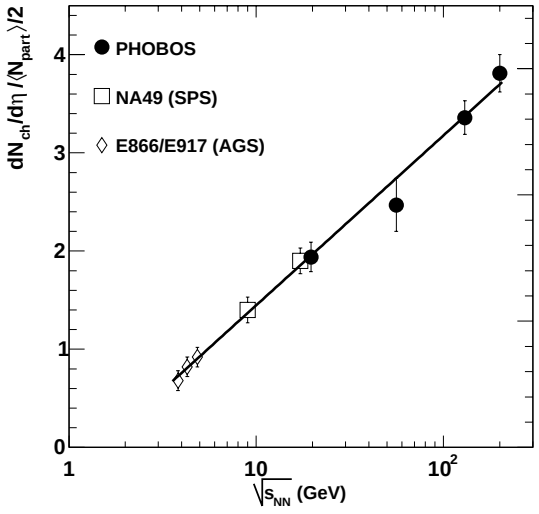

Fig. 1. Evolution of the midrapidity charged particle density $dN_{ch}/d\eta\rfloor_{|\eta|\leq 1}$, per participating nucleon pair, $N_{part}/2$, for central Au+Au (RHIC, AGS) and Pb+Pb (SPS) as a function of collision energy. Solid line is a logarithmic extrapolation of the data from lower energies drawn to guide the eye.

3. Baryon chemical potential at RHIC energies: Approaching a baryon free environment

One of the most interesting results from heavy-ion collisions at lower energies was the observation that the production ratios for different particles with cross-section varying over several orders of magnitude can be described in terms of a statistical picture of particle production assuming chemical equilibrium [7]. One of the key components in the particle production mechanism is the baryon chemical potential

μ_B which can be extracted from the K^+ to K^- and proton to antiproton ratios. The measurement of the ratios of charged antiparticles to particles produced at RHIC is shown in Fig. 2. This figure, taken from Ref. [8], compares the antiparticle to particle ratios for both kaons and protons to the corresponding data at lower energies.

The system formed at RHIC is closer to having an equal number of particles and antiparticles than that found at lower energies. The measured ratio for antiproton to proton production as function of the energy indicates that the system approaches smaller values of μ_B at higher energies showing that the system created at RHIC is close to a baryon-free medium. Assuming a hadronization temperature of 160–170 MeV, a value of $\mu_B = 27$ MeV was found for central Au+Au collisions at $\sqrt{s_{NN}}$=200 GeV.

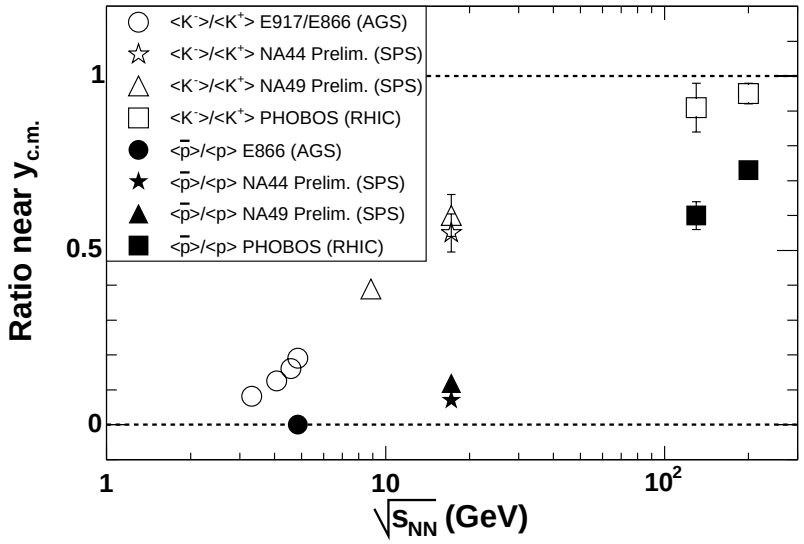

Fig. 2. Ratios of identified antiparticles over particles measured near midrapidity in central collisions of Au+Au (RHIC, AGS) and Pb+Pb (SPS) as a function of nucleon-nucleon center-of-mass energy. Error bars are statistical only.

4. Interaction strength in high energy density medium and evidence of thermalization

Figure 3 shows the magnitude of elliptic flow (v_2) measured by PHOBOS around midrapidity ($|\eta| \leq 1$) in Au+Au collisions at $\sqrt{s_{NN}}$=130 GeV and 200 GeV as a

function of the number of participants (N_{part}) [9, 10]. The elliptic flow signal is strong over a wide range in centrality and close to the value predicted by a relativistic hydrodynamics calculation [13], an indication of a certain degree of thermalization. The observation of an azimuthal asymmetry in the out-going particles is evidence of early interactions. Furthermore, from the strength of the observed elliptic flow and the known dimensions of the overlap region it can be estimated that the initially-formed medium equilibrates in a time less than about 2 fm/c [11], the value used earlier in the calculation of the energy density.

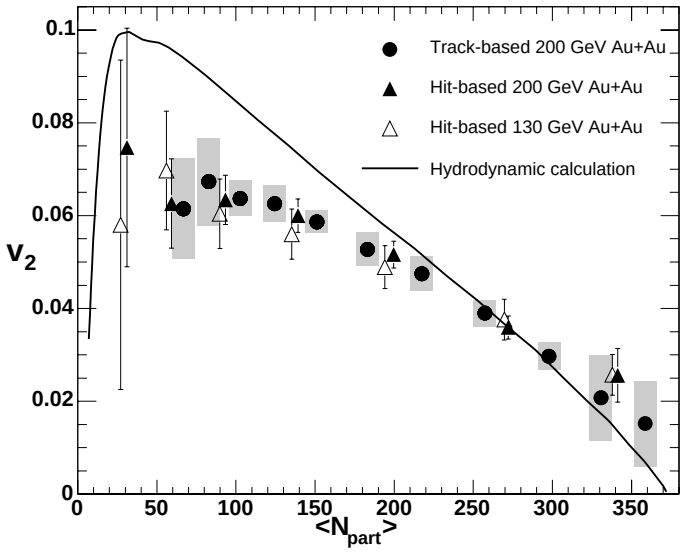

Fig. 3. Elliptic flow of charged particles near midrapidity ($|\eta| < 1$) as a function of centrality in Au+Au collisions at $\sqrt{s_{NN}}$=200 GeV (closed circles and triangles, are measurement using two different analysis methods) and at $\sqrt{s_{NN}}$=130 GeV (open triangles). Grey boxes show the systematic errors (90% C.L.) for the 200 GeV data. The curve shows the prediction from a relativistic hydrodynamics calculation.

Figure 4 shows the yield of charged particles per participant pair divided by a fit to the invariant cross section for proton-antiproton collisions [12] as a function of p_T, for peripheral (45-50% cross section) and central (0-6%) interactions. The dashed and solid lines show the expectation of the scaling of yields with the number of collisions (N_{coll}) and the number of participants (N_{part}), respectively. The brackets show the systematic uncertainty. We can see that the general shape of the curves is only weakly dependent on the centrality. More importantly, in each centrality bin, there is an increase of the yield in Au+Au collisions compared to $p\bar{p}$ at low

transverse momenta and a decrease in the relative yields above 2 GeV/c.

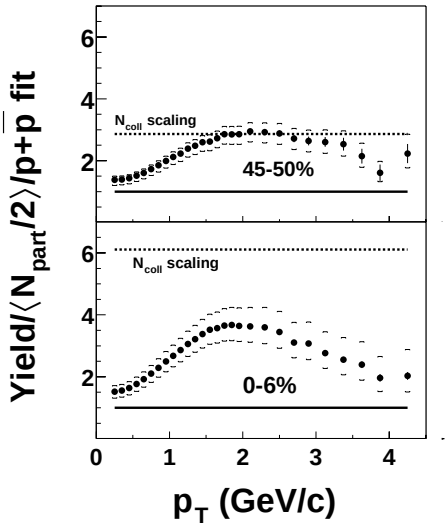

Fig. 4. Ratio of the yield of charged hadrons in Au+Au as a function of p_T for the most peripheral and most central bin to a fit of proton antiproton data scaled by $\langle N_{part}/2\rangle$. The dashed (solid) lines show the expectation of $N_{coll}(N_{part})$ scaling relative to p$\bar{\text{p}}$ collisions. The brackets show the systematic uncertainty.

Two possible explanations have been suggested for the yield suppression as a function of transverse momentum. The first ("initial state") model suggests that the effect is due to a modification of the wave functions of the nucleons in the colliding ions. This produces an effective increase of the interaction length in such a way the nucleons in a nucleus will interact coherently with all the nucleons in the other nucleus in the longitudinal dimension [14]. This model predicts not only the yield quenching at high p_T, but also the scaling of the yield with the number of participants. The second ("final state") model suggests that the suppression is due to the energy loss of the partons traveling through the hot dense medium formed in the Au+Au collisions [15]. One way to discriminate between these models is to reduce the size of the hot and dense medium, by colliding d+Au instead of Au+Au. RHIC's 2003 run was dedicated mainly to d+Au collision at $\sqrt{s_{NN}} = 200$ GeV. Details of the analysis and a broader discussion of p_T spectra are given in Ref. [16].

The nuclear modification factor is defined as the ratio of the d+Au invariant cross section divided by the p$\bar{\text{p}}$ UA1 yield, scaled by the proton-antiproton invariant cross section (41 mb) and $\langle N_{coll}\rangle$. In Fig. 5 we present R_{dAu} as a function of p_T for

four centrality bins. For each centrality bin there is a rapid rise of R_{dAu}, reaching a maximum at around p_T= 2 GeV/c. For comparison, the R-factor is also plotted for the most central bin for Au+Au collisions at $\sqrt{s_{NN}} = 200$ GeV. In striking contrast to the behavior of R_{dAu}, R_{AuAu} increases initially as function of p_T but above 2 GeV/c it decreases sharply.

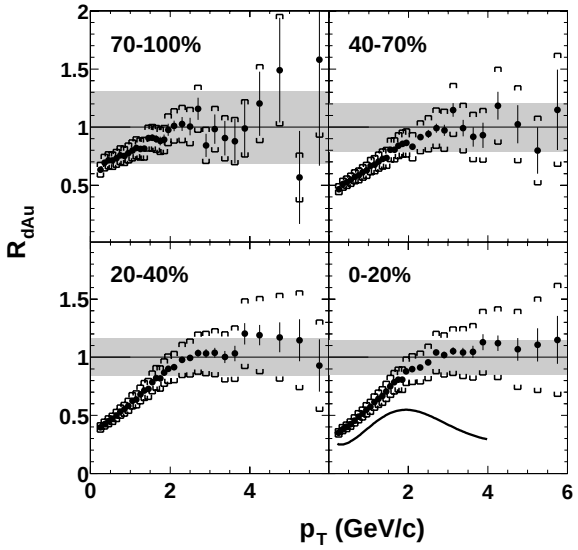

Fig. 5. Nuclear modification factor (R_{dAu}) as a function of p_T for four centrality bins. For the most central bin, (lower right) the spectral shape for central Au+Au data relative to $p + \bar{p}$ is shown for comparison. The shaded area shows the uncertainty in R_{dAu} due to the systematic uncertainty in $\langle N_{coll} \rangle$ and the UA1 scale error (90% C.L.). The brackets show the systematic uncertainty of the d+Au spectra measurement (90% C.L.).

The suppression of the inclusive yield observed in central Au+Au collisions is interpreted to be consistent with final-state interactions within a dense medium created in such collisions. Thus we find that the matter created at RHIC seems to interact strongly with high-p_T partons.

5. Global Observables

The range of systems and energies provided by RHIC has allowed the systematic study of the properties of particle production over a broad range of pseudorapidity and transverse momentum. Two global trends from this study have emerged, the

scaling of the yields with N_{part} and the extended longitudinal scaling behavior. Although a direct link between these observed trends in the data and the nature of the system created is not immediately obvious these features seem to reflect important aspects of the dynamics of the collisions.

5.1. N_{part} Scaling

The centrality dependence of the mid-rapidity yields has often been interpreted in a two-component picture of particle production with "soft" processes scaling with N_{part} and "hard" processes scaling with the number of binary collisions, N_{coll}. As the beam energy increases particle production from the hard processes is expected to dominate over that of soft processes [17]. This expectation is examined by studying the ratio of the yields at different energies at the same fraction of the cross section, as shown in Fig.6. The ratios are observed to be constant over the measured centrality range, showing a factorization of the centrality and beam energy dependences. Hence, the bulk particle production does not appear to exhibit the growing contribution from hard processes with collision energy.

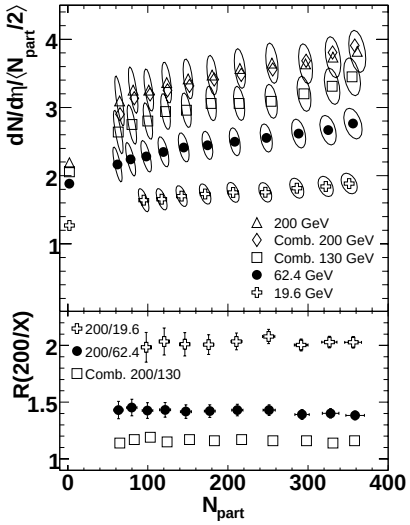

Fig. 6. The top panel is the Au+Au pseudorapidity distributions per participant pair at mid rapidity as a function of N_{part} for four energies. Also is shown the inelastic p+p data. The systematic errors are shown as 90% C.L. ellipses. The bottom panel is the ratio of the scaled pseudorapidity distributions.

5.2. Extended longitudinal scaling

The extended longitudinal scaling also referred as limiting fragmentation [5] is the invariance of the scaled pseudorapidity yields with beam energy in the reference frame of one of the projectiles, that is the scaled yields plotted as a function of $\eta' = \eta - y_{beam}$, where y_{beam} is the beam rapidity. Extended longitudinal scaling is shown for the Au+Au data in Fig. 7. This scaling is also found in d+Au collisions [18].

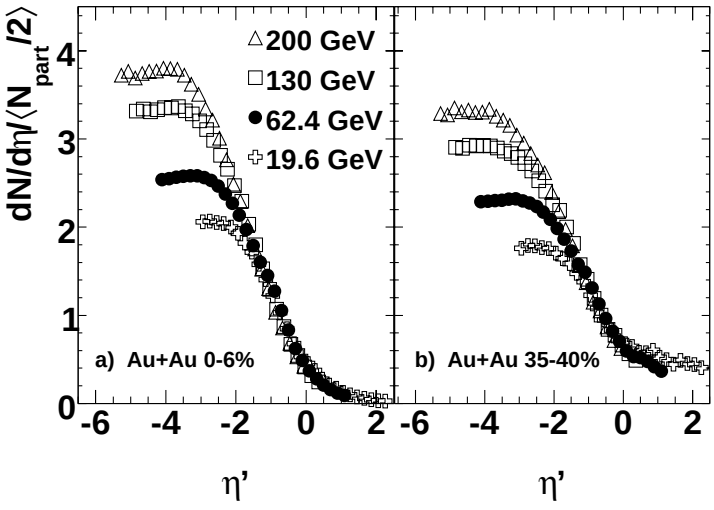

Fig. 7. Scaled pseudorapidity distribution per participant pair for two centrality bins and four energies as a function of the eta of the rest frame of one of the projectiles $\eta' = \eta - y_{beam}$, where y_{beam} is the beam rapidity. For clarity the systematic errors are not shown in the figure, but can be found in Ref. [5].

6. Final Remarks

In central Au+Au collisions at the highest RHIC energies, a very high energy density medium is formed. Conservative estimates of its density give a lower bound of 3 GeV/fm^3. This is greater than hadronic densities and it is inappropriate to describe this medium in terms of hadronic degrees of freedom. The medium has been found to have a low baryon chemical potential and there is evidence of some degree of thermalization. Two global trends from the study of the data have emerged, the scaling of the yields with N_{part} and the phenomenon of extended longitudinal

scaling. We expect to find more general features that characterize the system formed in the collisions by analyzing the rest of the PHOBOS data including p+p and Cu+Cu datasets.

Acknowledgment(s)

This work was partially supported by U.S. DOE grants DE-AC02-98CH10886, DE-FG02-93ER40802, DE-FC02-94ER40818, DE-FG02 - 94ER40865, DE-FG02-99ER41099, and W-31-109-ENG-38, by U.S. NSF grants 9603486, 0072204, and 0245011, by Polish KBN grant 1-P03B-062-27(2004-2007), and by NSC of Taiwan Contract NSC 89-2112-M-008-024.

Notes

a. E-mail: ejgarcia@uic.edu

References

1. F. Karsch, *Nucl. Phys.* **A698**, 199 (2002).
2. B. B. Back *et. al.*, (PHOBOS), *Nucl. Inst. Meth.* **A499**, 603 (2003).
3. B. B. Back *et. al.*, (PHOBOS), *Phys. Rev.* **C70**, 021902(R) (2004).
4. B. B. Back *et. al.*, (PHOBOS), *Nucl. Phys* **A757**, 28 (2005).
5. B. B. Back *et. al.*, (PHOBOS), *Phys. Rev. Lett.* **91**, 052303 (2003).
6. B. B. Back *et. al.*, (PHOBOS), *Phys. Rev.* **C70**, 051901(R) (2004).
7. P. Braun-Munzinger *et. al.*, *Phys. Lett. B* **465**, 15 (1999).
8. B. B. Back *et. al.*, (PHOBOS), *Phys. Rev. Lett.* **87** 102301 (2001).
9. B. B. Back, *et. al.*, (PHOBOS), *Phys. Rev. Lett.* **89** 222031 (2002).
10. B. B. Back, *et. al.*, (PHOBOS), submitted to *Phys. Rev. C (RC)*; arXiv:nucl-ex/0407012 (2004).
11. P. F. Kolb and U. Heinz, Hydrodinamical description of ultrarelativistic heavy ion collisions. *World Scientific* (2004); arXiv:nucl-th/0305084 (2003).
12. G. Arnison, et al., (UA1), Phys. Lett. B 118 (1982) 167.
13. U. W. Heinz, and H. Heiselberg, *Phys. Lett.* **500**, 232 (2001).
14. D. Kharzeev, E. Levin and L. McLerran, arXiv:hep-ex/0210332 (2002).
15. M. Gyulassy, I. Vitev, X. Wang and B. Zhang arXiv:hep-ex/0302077 (2003).
16. B. B. Back, *et. al.*, (PHOBOS), *Phys. Rev. Lett.* **91** 072302 (2003).
17. M. Gyulassy and X. N. Wang, *Comput. Phys. Commun.* **83**, 307, (1994).
18. B. Back, *et. al.*, (PHOBOS), *Phys. Rev.* **C72**, 031901(R) (2005).